Ab initio molecular dynamics simulation of hydrogen diffusion in α-iron

J. Sanchez,[1] J. Fullea,[1] M. C. Andrade,[1] and P. L. de Andres[2]

[1]*Instituto de Ciencias de la Construccion Eduardo Torroja, c/ Serrano Galvache 4, Madrid, Spain*
[2]*Instituto de Ciencia de Materiales de Madrid, Consejo Superior de Investigaciones Cientificas, Madrid, Spain*

First-principles atomistic molecular-dynamics simulation in the microcanonical and canonical ensembles has been used to study the diffusion of interstitial hydrogen in α-iron. Hydrogen to iron ratios between $\theta = \frac{1}{16}$ and $\frac{1}{2}$ have been considered by locating interstitial hydrogen atoms at random positions in a $2 \times 2 \times 2$ supercell. We find that the average optimum absorption site and the barrier for diffusion depend on the concentration of interstitials. Iron Debye temperature decreases monotonically for increasing concentration of interstitial hydrogen, proving that iron-iron interatomic potential is significantly weakened in the presence of a large number of diffusing hydrogen atoms.

Diffusion of hydrogen atoms in metals make an impact on a number of technologically important properties of the host material and has attracted interest since long ago.[1] In particular, it is believed to play a crucial role in embrittlement of high-strength steels, of common use in buildings, bridges, etc.[2-5] However, a fundamental understanding of different mechanisms-linking embrittlement and diffusion of hydrogen is still lacking owing to the complexity of the relevant processes. Different authors have used density-functional theory (DFT) to study preferred adsorption sites and diffusion barriers for hydrogen in body-center cubic iron (α-Fe), which constitutes the core of high-strength steels and consequently is the simplest model for fundamental studies trying to connect macroscopic and microscopic properties.[6-9] The main stream in the literature favors diffusion barriers of ≈ 0.1 eV and adsorption of hydrogen in the tetrahedral site which is the mot favorable one simply in terms of available space. Comprehensive work along these lines, including the effect of surfaces, has been done by Jiang and Carter,[10] and more recently Ramasubramaniam *et al.*[11] For large concentrations, however, we have found that occupancy of the competing octahedral site, and reduced diffusion barriers, can happen.[12] This is accompanied by a tetragonal distortion in the bcc unit cell and it is related to internal stresses appearing upon an increasing hydrogen load inside the system. From an experimental point of view, it has been observed that for increasing external pressures of hydrogen the iron-melting point is lowered appreciably and the transition from α (bcc) to γ (fcc) happens at lower temperature.[13] Furthermore, neutron-diffraction analysis on ferrite samples of high-strength steels have revealed a significant increase in Debye-Waller factors upon increasing loads of hydrogen.[14] In this Brief Report we investigate the effect of accumulating interstitial atoms in a region, which is known to happen at least locally around defects prior to the breaking of samples. We use *ab initio* molecular dynamics because it presents several advantages to study this problem. First, it allows us to study the many-body interactions between simultaneously diffusing interstitial impurities. Second, temperature-dependent simulations allow us to extract useful additional dynamical information. Third, for such a complex situation where the number of possibilities to distribute a number of interstitial impurities among several candidate sites becomes combina-

torially large, a statistical approach where the system follows its own internal dynamics to sample relevant configurations is the more effective approach. Kinetic Monte Carlo has also been recently applied to study the variation in barriers with different configurations and their associated stresses:[11] this is an alternative approach where good agreement with prior *ab initio* DFT calculations has been found, proving the viability of statistical methods to study this kind of problem.

First-principles molecular dynamics (MD) calculations have been performed with the CASTEP code.[15,16] A $2 \times 2 \times 2$ periodic supercell is set up including 16 Fe atoms and several H atoms depending on the different concentrations being considered. The Born-Oppenheimer approximation is used; ions are considered classical objects moving on the potential created by the electrons obeying the Schrödinger equation. Electronic wave functions are expanded using a plane-wave-basis set up to an energy cutoff of 375 eV and are sampled inside the Brillouin zone in a $4 \times 4 \times 4$ Monkhorst-Pack mesh.[17] Electronic energies are converged up to 10^{-5} eV. Ultrasoft pseudopotentials are used to describe Fe and H (Ref. 18) and the generalized gradients approximation for exchange and correlation due to Perdew, Burke, and Ernzerhof is chosen.[19] These approximation have been thoroughly checked before and it has been found that they reproduce correctly the main physical properties of α-iron, including lattice constant, magnetization, and bulk modulus.[12] The k-point mesh we are using in this Brief Report is less dense than the ones we have previously shown to be adequate to accurately reproduce different equilibrium properties of α-iron at $T=0$ K. Our choice is based in two different reasons. First of all, it is a practical one since *ab initio* molecular dynamics is a computer intensive task and a compromise between accuracy and time must be made. Second, we notice that computing different physical magnitudes require different accuracies. Figure 2 in Ref. 12 shows that a k-point mesh similar to the one we are using here incurs in a fractional error of 0.4% for the equilibrium lattice constant but $\approx 300\%$ for the bulk modulus. Presently, we focus in the calculation of total energies that fluctuate in the current range of temperatures by ≈ 0.05 eV. We have checked that for the maximum density of interstitial impurities considered here the total energy changes at $T=0$ K by 0.047 eV if the $4 \times 4 \times 4$ mesh is replaced by a $8 \times 8 \times 8$ one. Therefore, the error

becomes acceptable because it is similar to the random fluctuations intrinsic to the system. On the other hand, we notice that the error in the equilibrium lattice parameter by introducing such an approximation is ≈ 0.01 Å (e.g., Fig. 2 in Ref. 12), which is of the same order of magnitude or lower than the root-mean-squared amplitude displacements of vibrating atoms at the temperatures used here. Finally, we have checked our ability to reproduce the experimental value for the Debye temperature of bcc iron ($\Theta = 420$ K), a physical magnitude that will be used below to get physical insight from the molecular dynamics runs. We have obtained a theoretical value of $\Theta = 505$ K, quite acceptable for our purposes, in particular, because our methodology relies more than on absolute values on interpreting differences in magnitudes computed theoretically with the same parameters where a common background error should tend to cancel. Therefore, we conclude that the $4 \times 4 \times 4$ mesh is both practical and accurate enough for the purpose of these simulations.

To study the diffusion of several H atoms inside the unit cell we test in the microcanonical ensemble the quality of the total energy conservation during a typical MD run. Simulations for 1 or 2 ps are performed with time steps of 0.5 or 1.0 fs showing that the total energy is conserved within a 0.01% error (equilibration taking place during the first 100–200 fs have been taken out from averages). Keeping fixed the parameters defining the model, we switch to the canonical ensemble to reproduce conditions where the Fe and H atoms are in equilibrium with a thermal bath kept at a fixed temperature (Nose-Hover prescription has been used). All these simulations are performed keeping constant the volume of the unit cell and the number of particles. These boundary conditions are important to understand the physical model and the solutions obtained. In particular, it is relevant to discuss the meaning of keeping the volume fixed. In a previous work we have investigated the volume deformation and atomic displacements necessary to find an equilibrium solution with zero forces and stresses in the presence of interstitial hydrogen binding to either the octahedral or tetrahedral high-symmetry sites.[12] Here we are interested, for the case of an overall low dilution concentration of impurities, in the effect of a high concentration of interstitial atoms inside a small region embedded in a matrix of iron that, except for the large concentration of interstitial hydrogen in a small number of regions, mostly keeps its original properties. This is consistent with the experimental observation of overall low dilution of interstitial H in α-iron, but possibly large concentration in particular regions, maybe as a consequence of the existence of defects.[1,14] Therefore, we assume that the modification of the volume in the region of interest due to the internal pressure created by the impurities is effectively controlled by the larger amount of unperturbed bulk material surrounding the region where the interstitial hydrogen diffuses in a scale of time compatible with our simulations (ps). Consequently, we keep the simulation $2 \times 2 \times 2$ supercell volume fixed, equal to the one corresponding to α-iron. Other models might be of interest for different conditions: e.g., a large and uniform concentration of impurities. This would require adjusting the volume for each density. We estimate that for this case the volume would change between
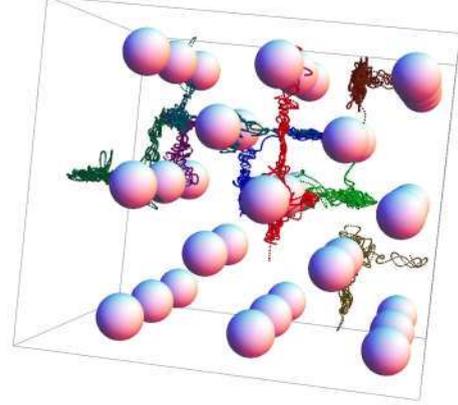

FIG. 1. (Color online) Simulated random walks ($T = 700$ K) for eight interstitial hydrogen atoms simultaneously located in a $2 \times 2 \times 2$ bcc supercell.

5% and 15% in the range of impurity concentrations considered in this work. While the (NVE) and (NVT) collectives are appropriate for the first scenario above, for the second one the (NPH) and (NPT) collectives should be used. The (NPH) and (NPT) collectives would also be more adequate to describe the region near the surface, where the lattice of iron breaks its periodicity and might not be able to counteract the internal pressure due to impurities and the volume could change. This work follows closely the first scenario, making use of the (NVE) and (NVT) collectives only.

Diffusion coefficients are computed by assuming a random walk for interstitial impurities.[20] Fig. 1 shows the different paths for the high-density case with eight hydrogen atoms diffusing simultaneously inside the $2 \times 2 \times 2$ supercell. As already predicted by our static geometry optimization interstitial hydrogen atoms avoid each other and no tendency to formation of molecular hydrogen has been observed. We follow the different trajectories during the simulation time and compute averages

$$\langle |r(t) - r(0)|^2 \rangle = 6Dt \quad (1)$$

to extract the three-dimensional diffusion coefficient D. Barriers for diffusion are estimated from an Arrhenius plot $D = D_0 e^{-B/k_B T}$ by a least-squares fit. Here, the prefactor D_0 is related to a typical vibrational frequency for H in the Fe bcc lattice, and it is assumed to be a constant value independent of the number of interstitial atoms in the supercell. This assumption is corroborated by our fits within an uncertainty of $\pm 12\%$ (Fig. 2).

We simulate MD trajectories for a single H atom diffusing inside the supercell to compare with previous results derived from *ab initio* DFT geometrical optimization and transition state theory. From a least-squares fit to the data in the Arrhenius plot we determine a barrier for diffusion $B_1 = 0.145$ eV (Fig. 2) in good agreement with previous values obtained under similar conditions (cubic symmetry and the same interstitial density[12]). This agreement shows that our MD simulations adequately sample the relevant phase space. The time evolution of the interstitial atom can be further analyzed to show that under these conditions trajectories
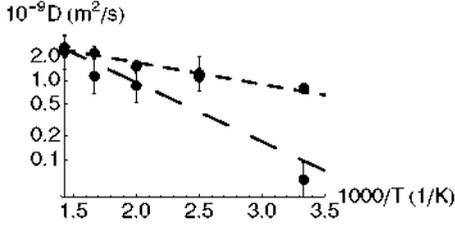
FIG. 2. (a) (Short dashed line) Diffusion coefficient, D ($\frac{m^2}{s}$), obtained for a set of averaged diffusion MD trajectories for a single H atom in a $2 \times 2 \times 2$ bcc iron supercell. A barrier for diffusion of $B_1 = 0.145$ eV is obtained from a least-squares fit. (b) (Long dashed line) Same for eight H interstitial atoms diffusing in the supercell. A barrier of $B_8 = 0.047$ eV is deduced from the fit. Error bars have been estimated from standard errors ($\frac{1.96\sigma}{\sqrt{N}}$).

near tetragonal sites (T) are preferred over octahedral sites (O). This conclusion can be made quantitative by computing a characteristic residence time for both sites. We assign parts of the diffusing path either to T or O according to proximity to estimate the likelihood to find the particle, say, near O. Figure 3 displays the fractional occupation of octahedral sites for one, two, four, and eight hydrogen atoms in the $2 \times 2 \times 2$ supercell. These values can be understood by comparing with a simple two-level model where the only parameter is the energy difference between T and O sites, $k_B \Delta = E_O - E_T$ (Ref. 21)

$$\frac{O}{O + T} = \frac{1}{1 + 2e^{\Delta/T}}. \tag{2}$$

This model reduces all the accessible volume for the interstitial hydrogen diffusing in the unit cell to only a set of discrete lattice points (either T or O) but in spite of its crudeness it already captures the essentials of the problem. Equation (2) has been plotted in Fig. 3 for $k_B \Delta = 0.06$, 0.07, 0.04, and -0.035 eV, yielding least-squares fits to the points extracted from the MD simulations for $n_H = 1$, 2, 4, and 8 interstitial hydrogen atoms, respectively. The dashed line represents the asymptotic equilibrium distribution ($O_{T \to \infty} = \frac{1}{3}$) to be approached from above or below depending on the sign of
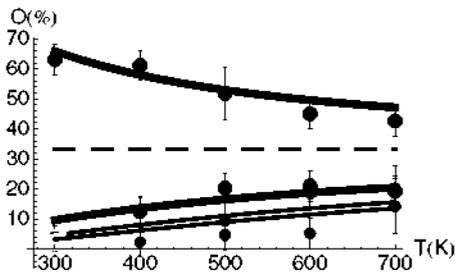

FIG. 3. As a percentage over the total simulation time, residence time around octahedral sites, P_O for: (i) a single interstitial hydrogen [small gray dots; thin gray line corresponds to $k_B \Delta = 0.06$ eV in Eq. (2)]; (ii) two H (small black dots; thin black line is for $k_B \Delta = 0.07$ eV); (iii) four H (large gray dots; thick gray line is for $k_B \Delta = 0.04$ eV); and (iv) eight H (large black dots; thick black line is for $k_B \Delta = -0.035$ eV). The dashed line separates the two asymptotic regions ($\Delta \geq 0$ and $\Delta \leq 0$).

Δ. These results show that for $n_H = 8$ ($\theta = \frac{1}{2}$) Δ has moved from positive to negative and the equilibrium site has been exchanged from T to O. The dependence of the parameter Δ with the interstitial density proves how site-adsorption energies are affected by the presence of an increasing number of hydrogen atoms concentrated in a particular region. This behavior follows the pattern previously predicted by ab initio DFT geometry optimization where the T site is the lowest-energy configuration for low densities while for large densities occupancy of the O site favors a body-centered tetragonal distortion of the lattice and becomes the global minimum. Although for the γ phase, experiments reporting a qualitative modification of the system around a hydrogen concentration of ≈ 0.4 show how the increasing density of interstitial impurities might significantly modify the dynamics of these systems (e.g., Fig. 13 in Ref. 13). This is an observation that might help to explain the spreading of values extracted from different experimental techniques for diffusion barriers that has previously been linked to partial occupation of both sites.[22] Partial occupation of both sites at a given temperature happens most naturally in molecular dynamics simulations but it is not easy to describe in a standard geometry optimization. We remark that the present approach represents a feasible route to investigate a regime that otherwise is too difficult: in the $2 \times 2 \times 2$ there are 48 different O sites and 96 different T sites, being the number of ways to distribute several interstitial among these combinatorially large ($\approx 10^{11}$). Such a huge configurational space can only be addressed from a statistical point of view and by letting the system to explore as many relevant cases as possible by following its own dynamics. To understand to which extent barriers for diffusion are affected by the presence of extra interstitial atoms we analyze the high-density case $\theta = \frac{1}{2}$ in more detail. From an Arrhenius plot (Fig. 2) we extract by a least-squares fit an effective barrier of $B_8 = 0.047$ eV; significantly lower than the one found for a single interstitial, B_1.

Based in ab initio DFT geometrical optimization we have previously suggested that an important consequence of interstitial hydrogen diffusing in α-Fe is to weaken the Fe-Fe interaction.[12] From a physical point of view this effect is related to several factors: first, interstitial impurities help to screen the Fe-Fe interaction; second, the symmetry is distorted, an effect that is important to explain the stability of octahedral sites versus tetrahedral ones in the high-density regime; third, spin-polarized DFT calculations reveal that hydrogen contributes an extra spin to the system, but the total ferromagnetic moment does not grow accordingly, which we interpret as a weakening of electronic interactions. Current MD simulations should be interpreted as controlled and clean theoretical experiments that help to explore new domains, such as nonzero temperatures, or the collective behavior of a large number of interstitial impurities meeting together in the same region. We remark that our MD simulations support similar physical interpretations as the ones derived from ab initio DFT at $T = 0$ K. We compute the mean-square amplitudes of iron atoms vibrating around their equilibrium positions, $\langle u^2 \rangle$, which is related to the strength of the potential confining these atoms. For each temperature we obtain the mean-squared amplitude of vibration by fitting their time-averaged probabilities to a Gaussian distribution
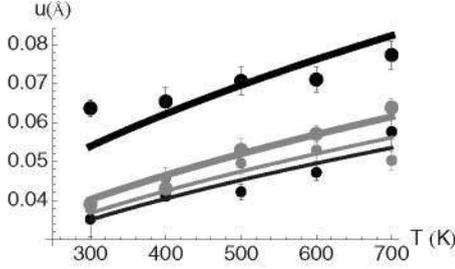
FIG. 4. Iron root-mean-squared displacement from equilibrium positions $u(\text{Å})$ vs temperature (K). The density of interstitial hydrogen for each case is: (i) $n_H=1$ (small gray dots), (ii) $n_H=2$ (small black dots), (iii) $n_H=4$ (large gray dots), and (iv) $n_H=8$ (large black dots). Corresponding continuous lines coded similarly in size and gray/black are least-square fits to the data using Eq. (3) with Debye temperatures $\Theta=381$, 399, 360, and 259 K, respectively.

centered around its equilibrium position. These values are compared with an isotropic Debye-Waller model for the mean-squared displacement of atoms vibrating at temperature T (Ref. 23)

$$\langle u^2 \rangle = \frac{3\hbar^2}{4k_B M\Theta}\left(\frac{T}{\Theta}\int_0^{\Theta/T} \frac{x\,dx}{e^x-1} + \frac{1}{4} \right), \qquad (3)$$

where Θ is the Debye temperature and M the mass of the atom. Figure 4 shows how the root-mean-squared amplitude of vibration (u) increases steadily with the number of H atoms inside the $2\times2\times2$ supercell, being nearly doubled from $n_H=1$ to 8. Adopting a Lindemann-type criterion we can conclude that increasing the number of interstitial hydrogen drives the material closer to a thermodynamic instability that eventually should lead either to a phase transition or to the material failure. This idea is more clearly illustrated by using Eq. (3) to fit these $\langle u^2 \rangle$ to an effective Debye temperature for each density (Fig. 5). Θ decreases monotonously when the number of interstitial hydrogen atoms increases marking the softening of α-iron and proving that the material
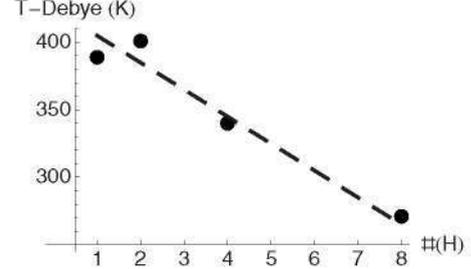

FIG. 5. Debye-Waller temperature (K) vs number of interstitial H diffusing in the unit cell. Dashed line is a linear least-squares fit to guide the eye.

is, at a given fixed T, getting closer to its own melting point under the internal pressure of dissolved H. This is closely related to the growing number of interstitial atoms sitting together in the same unit cell. The inverse situation (growing temperature getting closer to the melting point at a fixed number of interstitial impurities) cannot be inferred from our simulations because the Debye Temperature is constant under these conditions.

We have found by direct analysis of our MD trajectories that the diffusing barrier for interstitial hydrogen inside α-iron depends on the density of diffusing atoms in the near region. By using a simple statistical model we have also analyzed how the energy difference between the T and O sites, Δ, is modified by the presence of other interstitials. Finally, by looking at the amplitude of vibration of iron atoms around their equilibrium position and comparing with a simple Debye-Waller model, we conclude that the Fe-Fe interaction weakens as the concentration of interstitial hydrogen increases, finding that for the largest considered density the effective Debye temperature for iron is already below room temperature.

[1] G. Alefeld and J. Volkl, *Hydrogen in Metals I and II—Application-oriented Properties*, Topics in Applied Physics (Springer-Verlag, Berlin, 1978), Vol. 28.

[2] N. Eliaz, A. Shachar, B. Tal, and D. Eliezer, Eng. Failure Anal. **9**, 167 (2002).

[3] Y. Liang, P. Sofronis, and N. Aravas, Acta Mater. **51**, 2717 (2003).

[4] M. Elices, J. Ruiz, and J. M. Atienza, Mater. Struct. **37**, 305 (2004).

[5] D. M. Li, R. P. Gangloff, and J. R. Scully, Metall. Mater. Trans. A **35**, 849 (2004).

[6] J. K. Nørskov, Phys. Rev. B **26**, 2875 (1982).

[7] X. G. Gong, Z. Zeng, and Q. Q. Zheng, J. Phys.: Condens. Matter **1**, 7577 (1989).

[8] C. Elsässer, J. Zhu, S. G. Louie, M. Fahnle, and C. T. Chan, J. Phys.: Condens. Matter **10**, 5081 (1998).

[9] A. Juan and R. Hoffmann, Surf. Sci. **421**, 1 (1999).

[10] D. E. Jiang and E. A. Carter, Phys. Rev. B **70**, 064102 (2004).

[11] A. Ramasubramaniam, M. Itakura, M. Ortiz, and E. A. Carter, J. Mater. Res. **23**, 2757 (2008).

[12] J. Sanchez, J. Fullea, C. Andrade, and P. L. de Andres, Phys. Rev. B **78**, 014113 (2008).

[13] Y. Fukai, J. Alloys Compd. **404-406**, 7 (2005).

[14] M. Castellote *et al.*, Nucl. Instrum. Methods Phys. Res. B **259**, 975 (2007).

[15] S. J. Clark, M. D. Segall, C. J. Pickard, P. J. Hasnip, M. J. Probert, K. Refson, and M. C. Payne, Z. Kristallogr. **220**, 567 (2005).

[16] CASTEP 4.3; http://www.accelrys.com

[17] H. J. Monkhorst and J. D. Pack, Phys. Rev. B **13**, 5188 (1976).

[18] D. Vanderbilt, Phys. Rev. B **41**, 7892 (1990).

[19] J. P. Perdew, K. Burke, and M. Ernzerhof, Phys. Rev. Lett. **77**, 3865 (1996).

[20] H. Mehrer, *Diffusion in Solids* (Springer-Verlag, Berlin, 2007).

[21] W. G. W. Rosser, *Statistical Physics* (Wiley, New York, 1986).

[22] K. Kiuchi and R. B. McLellan, Acta Metall. **31**, 961 (1983).

[23] R. W. James, *The Optical Principles of the Diffraction of X-Rays* (Bell, London, 1962).